**Article:**

Taylor, LS orcid.org/0000-0001-7916-0856, Swindles, GT orcid.org/0000-0001-8039-1790, Morris, PJ orcid.org/0000-0002-1145-1478 et al. (2 more authors) (2019) Evidence for ecosystem state shifts in Alaskan continuous permafrost peatlands in response to recent warming. Quaternary Science Reviews, 207. pp. 134-144. ISSN 0277-3791

https://doi.org/10.1016/j.quascirev.2019.02.001

# Evidence for ecosystem state shifts in Alaskan continuous permafrost peatlands in response to recent warming

Liam S. Taylor[1], Graeme T. Swindles[1,2], Paul J. Morris[1], Mariusz Gałka[3], Sophie M. Green[4]

[1] School of Geography, University of Leeds, Leeds, UK

[2] Ottawa-Carleton Geoscience Centre and Department of Earth Sciences, Carleton University, Ottawa, Ontario, Canada

[3] Department of Geobotany and Plant Ecology, Faculty of Biology and Environmental Protection, University of Lodz, Lodz, Poland

[4] Geography, College of Life and Environmental Sciences, University of Exeter, Exeter, UK

**Corresponding Author:** Liam Taylor, gylst@leeds.ac.uk

**Key Words:** Arctic; Climate Change; Holocene; Hydrology; Testate Amoebae; Reconstruction

**Highlights:**

- Reconstruction of late-Holocene environmental change from Alaskan peatlands
- Apparent increase in carbon accumulation rates since ~1850 CE
- Shift towards dry, oligotrophic states under post-1850 warming
- Some permafrost peatlands may accumulate carbon more rapidly under future warming

**Abstract:**

Peatlands in continuous permafrost regions represent a globally-important store of organic carbon, the stability of which is thought to be at risk under future climatic warming. To better understand how these ecosystems may change in a warmer future, we use a palaeoenvironmental approach to reconstruct changes in two peatlands near Toolik Lake on Alaska's North Slope (TFS1 and TFS2). We present the first testate amoeba-based reconstructions from peatlands in continuous permafrost, which we use to infer changes in water-table depth and porewater electrical conductivity during the past two millennia. TFS1 likely initiated during a warm period between 0 and 300 CE. Throughout the late-Holocene, both peatlands were minerotrophic fens with low carbon accumulation rates (means of 18.4 and 14.2 g C $m^{-2}$ $yr^{-1}$ for cores TFS1 and TFS2 respectively). However, since the end of the Little Ice Age, both fens have undergone a rapid transition towards oligotrophic peatlands, with deeper water tables and increased carbon accumulation rates (means of 59.5 and 48.2 g C $m^{-2}$ $yr^{-1}$ for TFS1 and TFS2 respectively). We identify that recent warming has led to these two Alaskan rich fens to transition into poor fens, with greatly enhanced carbon accumulation rates. Our work demonstrates that some Arctic peatlands may become more productive with future regional warming, subsequently increasing their ability to sequester carbon.

## 1. Introduction

### 1.1. Background

Peatlands in the continuous permafrost zone are globally-important stores of ~144 Pg of organic carbon (Tarnocai et al., 2009). The stability of this carbon store is thought to be threatened by current and future warming of the high-latitudes (Khvorostyanov et al., 2008; Schuur et al., 2008; Schuur et al., 2013), although the ultimate fate of permafrost peatlands and their ability to sequester carbon under future warming are uncertain. Under projected warming, land surface models suggest that the Arctic will become a net carbon source by the mid-2020s as a direct result of the degradation of permafrost and subsequent release of carbon (Schaefer et al., 2011). The potential for greenhouse gas production from peatlands is likely to increase under future climate change (Hodgkins et al., 2014), particularly during dry periods when falling water tables are likely to expose peat to rapid, aerobic decomposition, leading in turn to elevated carbon dioxide ($CO_2$) release (Ise et al., 2008). However, permafrost thaw may instead lead to wetter surface conditions, thereby releasing more methane ($CH_4$) from anaerobic decomposition (Moore et al., 1998). Net primary productivity in peatlands is likely to rise due to longer, warmer growing seasons, and shifts towards more productive vegetation, which would enhance carbon accumulation (Natali et al., 2012), leading to a negative climate feedback. In all projections of future warming, Gallego-Sala et al. (2018) identify increased carbon sequestration in high-latitude peatlands. At present there remains no consensus on whether permafrost peatland carbon budgets will have net warming or cooling effects under future climate change.

Palaeoecological approaches have been used to identify how peatlands have responded to climate change during the late-Holocene (Langdon and Barber, 2005; Sillasoo et al., 2007; Swindles et al., 2007, 2010; Beaulieu-Andy et al., 2009; Gałka et al., 2017). It is sometimes possible to identify correlations between reconstructed hydrology and climate variables (e.g. temperature and precipitation), where there is precise chronological control for the recent (~1850 CE) part of the peat profile. In studies from the UK (Charman et al., 2004) and Estonia (Charman et al., 2009), precipitation has been shown to exert the strongest control on reconstructed water table, with temperature a second-order influence. Reconstructions over the late-Holocene also show that carbon accumulation is likely to increase with rising temperatures as a result of improved net primary productivity (Charman et al., 2013). Despite the importance of continuous permafrost peatlands as a carbon store, there have been no quantitative reconstructions to identify how the carbon dynamics of these systems have responded to Holocene climate change. Furthermore, there is a paucity of long-term monitoring of peatlands in the continuous permafrost zone. As a result, peatland response to recent warming is poorly understood in the high-latitudes.

Testate amoebae are single-celled protists that are sensitive hydrological indicators (Woodland et al., 1998). They are well preserved in peatlands, so can be used to reconstruct palaeohydrological metrics such as water table depth (WTD) over Holocene timescales. Testate amoeba-based reconstructions have been used in permafrost regions of Canada (Lamarre et al., 2012), Sweden (Swindles et al., 2015a), Finland and Siberia (Zhang et al., 2018), but their use has been limited to discontinuous and sporadic permafrost. We recently developed two new transfer functions from continuous permafrost peatlands across the Alaskan North Slope, which facilitate reconstruction of both WTD and porewater electrical conductivity (EC) during the Holocene, where EC can be used as a proxy for a peatland's trophic status along the fen-bog gradient (Taylor et al., 2019). By reconstructing Holocene hydrological change and calculating the carbon accumulation rate (CAR), we can begin to identify the environmental controls on these important variables in continuous permafrost peatlands. By doing so we seek to improve predictions about the likely future response of continuous permafrost peatlands, particularly the vulnerability of their carbon stores, to projected climatic warming.

### 1.2. Aim and Hypotheses

Our aim is to reconstruct palaeoenvironmental conditions from two Alaskan peatlands in the continuous permafrost zone. In this investigation, we:

i. Examine the palaeoecology of testate amoebae through the late-Holocene from two peatlands beside Toolik Lake, North Slope, Alaska;
ii. Reconstruct WTD, EC and CAR;
iii. Test whether CAR, WTD and EC have been controlled by changes in temperature and precipitation;;
iv. Compare these data to plant macrofossil records to identify changes in peatland vegetation alongside hydrological changes.

## 2. Methods

### 2.1 Study Area

Our study examines two cores (TFS1 and TFS2; Table 1), one each from the deepest peat in each of the two study sites, which extend to the bottom of the active layer. The cores come from two distinct peatlands approximately 250 metres apart and adjacent to Toolik Lake on the Alaskan North Slope. A bedrock high separates the watersheds of the two peatlands (Figure 1). The study area sits within the continuous permafrost region, with an active layer thickness of between 40 and 50 cm (Brown, 1998), and is surrounded by Arctic acidic tundra. Toolik Lake is situated in the northern foothills of the Brooks Mountains, at an elevation of approximately 712 m above sea level and is subject to a continental climate. Mean daily temperature ranges from 11℃ in the summer to -23℃ in winter with annual precipitation of ~250 mm (Environmental Data Center Team, 2018; averaging period 1988–2017). The region is snow free from early June to mid-September.

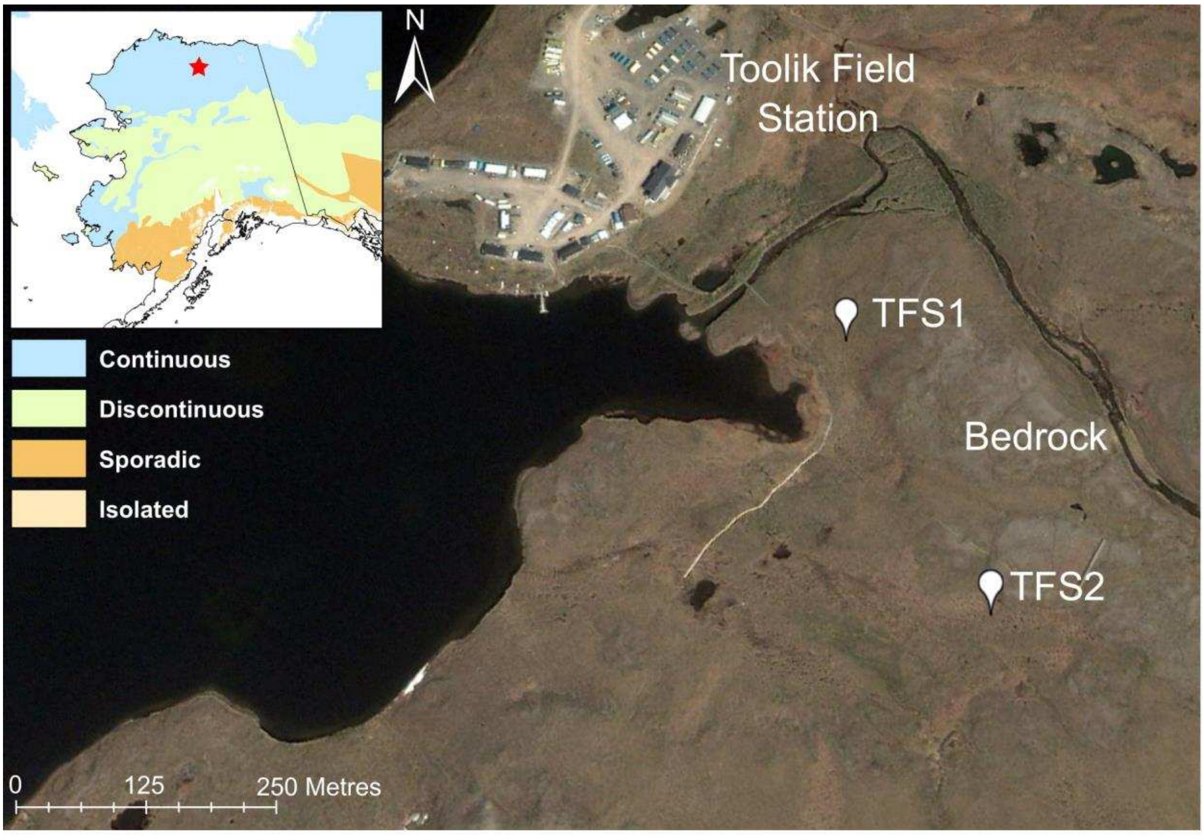


Figure 1 – Site Map. TFS1 and TFS2 are situated in peatlands to the south of Toolik Field Station, approximately 250 metres apart and separated by a bedrock high.

| Core | Co-ordinates | Core Length (cm) | Distance to lake shore (m) | Elevation above sea-level (m) | Approximate oldest age (CE) | Dominant surface vegetation |
|---|---|---|---|---|---|---|
| TFS1 | 68.62475, -149.59639 | 45 | 51 | 715 | 800 | Sphagnum fuscum, Sphagnum capillifolium, Andromeda poligolia, Betula nana |
| TFS2 | 68.62276, -149.60028 | 50 | 222 | 724 | 0 | Sphagnum capillifolium, Aulacomnium turgidum, Salix reticulata |

Table 1 – Information on cores TFS1 and TFS2.

## 2.2 Peat sampling and dating

We studied two short peat cores, TFS1 and TFS2, collected in July 2015 as 8 cm x 8 cm monoliths. For additional details on sampling, see Gałka et al. (2018). We sub-sampled both cores at contiguous 1 cm depth increments and created a chronology using radiocarbon dates previously reported by Gałka et al. (2018), with additional $^{210}$Pb dating. Gałka et al. (2018) carried out $^{14}$C dating using Accelerator Mass Spectrometry (AMS) on a combination of macrofossils and bulk peat, from five samples in each core, using OxCal 4.1 software and the IntCal13 curve to calibrate the radiocarbon dates. We used the same $^{14}$C dates as Gałka et al. (2018), with the exception of two dates that we omitted (TFS1 18-19 cm and TFS2 13-14 cm, corresponding to 1679-1940 CE and 1694-1919 CE respectively) because they fall within the range covered with our more precise $^{210}$Pb dating (post-1900 CE).

We measured $^{210}$Pb activity at 1 cm depth increments using alpha spectrometry by measuring the alpha decay of polonium-210 ($^{210}$Po), a daughter-product of $^{210}$Pb decay. Sub-samples of 0.5 g of peat were freeze-dried, ground and homogenised, and spiked with a $^{209}$Po chemical yield tracer. We extracted $^{210}$Po from the peat samples using a sequential $HNO_3$:$H_2O_2$:HCl (1:2:1) acid digestion, then electroplated onto silver planchets (based on Flynn, 1968). We measured the $^{209}$Po and $^{210}$Po activities using Ortec Octête Plus alpha spectrometers at the University of Exeter's Radiometry

Laboratory. We calculated ages using the Constant Rate of Supply (CRS) model (Appleby and Oldfield, 1978; Appleby, 2001). The main assumptions of the CRS model are: (1) a constant supply of $^{210}Pb$ to the peat surface; (2) rapid transfer of $^{210}Pb$ to peat; and (3) post-depositional immobility (Appleby, 2001). $^{210}Pb$ data and activity profiles are given in the Supplementary Material.

We combined $^{14}C$ and $^{210}Pb$ age determinations and used them to create a Bayesian age model for each core using R version 3.4.1 (R Core Team, 2014), and the rbacon package (version 2.3.4; Blaauw et al., 2018) (Figures 2a, b). Bacon uses a priori information of peat accumulation rate (20 yr cm$^{-1}$ for TFS1; 50 yr cm$^{-1}$ for TFS2), over multiple short sections of the core (1.5 cm) to produce flexible, robust chronologies (following Swindles et al., 2012). Using this a priori information, in addition to $^{210}Pb$ and $^{14}C$ dating, we modelled both cores to determine the maximum age probability for each 1 cm sub-sample to a maximum of 50 cm depth. Hereafter, all references to ages or years refer to the maximum age probability at a given depth, as determined from the age model, unless otherwise specified.

## 2.3 Carbon accumulation analysis

Sub-samples were examined at 1 cm depth increments, using samples of 2 cm$^3$. We measured and weighed each sub-sample, oven-dried overnight at 105℃, and re-weighed to determine gravimetric moisture content and dry bulk density (BD); and then ignited at 550℃ for at least 4 hours, and re-weighed again to determine organic matter content through loss-on-ignition (LOI). We used the assumption that the carbon content of peat is 50% of organic matter (measured by LOI; following Bellamy et al., 2005). CAR for each 1 cm interval was subsequently calculated as follows:

$$CAR = \frac{z}{T_a} \times BD \times C_c \times 100$$

Where CAR is carbon accumulation rate (g C m$^{-2}$ yr$^{-1}$), z is depth (cm), $T_a$ is age difference between the 1 cm interval and the sub-sample below, BD is dry bulk density (g cm$^{-3}$) and $C_c$ is carbon content (%).

## 2.4 Testate amoeba analysis

We isolated testate amoebae for analysis following Booth et al. (2010). Approximately 2 $cm^3$ of each sub-sample (at 1 cm intervals) was placed in freshly boiled water for 10 minutes, shaken, passed through a 300 μm sieve and back-sieved through a 15 μm mesh. We aimed to count at least 100 individuals at 200–400 × magnification under a high-power transmitted light microscope. Eleven samples from TFS1 had fewer than 100 individuals (min n = 81), while seven samples in TFS2 had fewer than 100 individuals (min n = 66). We omitted the deepest two samples in TFS2 from further analysis due to particularly low counts (n = 22 and 9 respectively), resulting from poor preservation. Testate amoebae were identified with the assistance of published guides (Charman et al., 2000; Booth and Sullivan, 2007; Siemensma, 2018). For the first time, we apply two modified transfer functions from continuous permafrost peatlands across the Alaskan North Slope (Taylor et al., 2019) to reconstruct WTD and EC.

## 2.5 Climate data

We extracted monthly temperature and precipitation records from 1901 to present from the CRU TS v. 4.01 dataset (Harris et al., 2014) for the grid cell centred on 68.75°N, 149.75°W. This dataset utilises 22 stations from across Alaska to interpolate climate data to half degree spatial resolution. All stations are land-based, with the nearest station to Toolik Lake being 217 km away at Bettles. This dataset has high accuracy when compared to equivalent data sources for Alaska (Harris et al., 2014). We used the PAGES2k Consortium (2017) Arctic database to reconstruct annual temperatures from 0 CE. PAGES2k is a multi-proxy dataset, predominantly using tree rings, marine sediments and glacier ice that range in temporal coverage. Tree rings make up the majority of the most recent temporal coverage, while marine sediments and glacier ice are used to reconstruct temperature back to 0 CE. For more details, see PAGES2k Consortium (2017). Change point analysis was performed on these climate data using the R changepoint package (version 2.2.2; Killick et al., 2016), following Amesbury et al. (2017). We used the cpt.mean function to identify the primary change of the mean within each time series. The time series of each variable was the full error range (min–max) of the date at the sub-sample interval from the respective age model.

## 3. Results

### 3.1 Age-depth model

The bottom of the active layer in TFS1 begins at c. 800 CE, while in TFS2 it is much older, dating to c. 0 CE (Figure 2). The use of high resolution $^{210}$Pb data result in an average ± 2–3 years error in reconstructing change from 1900 CE. Before 1900 CE, error increases beyond the range of $^{210}$Pb dating, where $^{14}$C dates are used. We follow Gałka et al. (2018) in rejecting a $^{14}$C date of bulk peat at the bottom of TFS2 (AMS dated to 950 ± 30 $^{14}$C BP, suggesting contamination), but this does introduce large uncertainty in the true age of peatland initiation in this core. Peat accumulation rate is slow (as expected in permafrost environments) throughout both cores, rapidly accelerating from the start of the industrial revolution (which we define as 1850 CE).

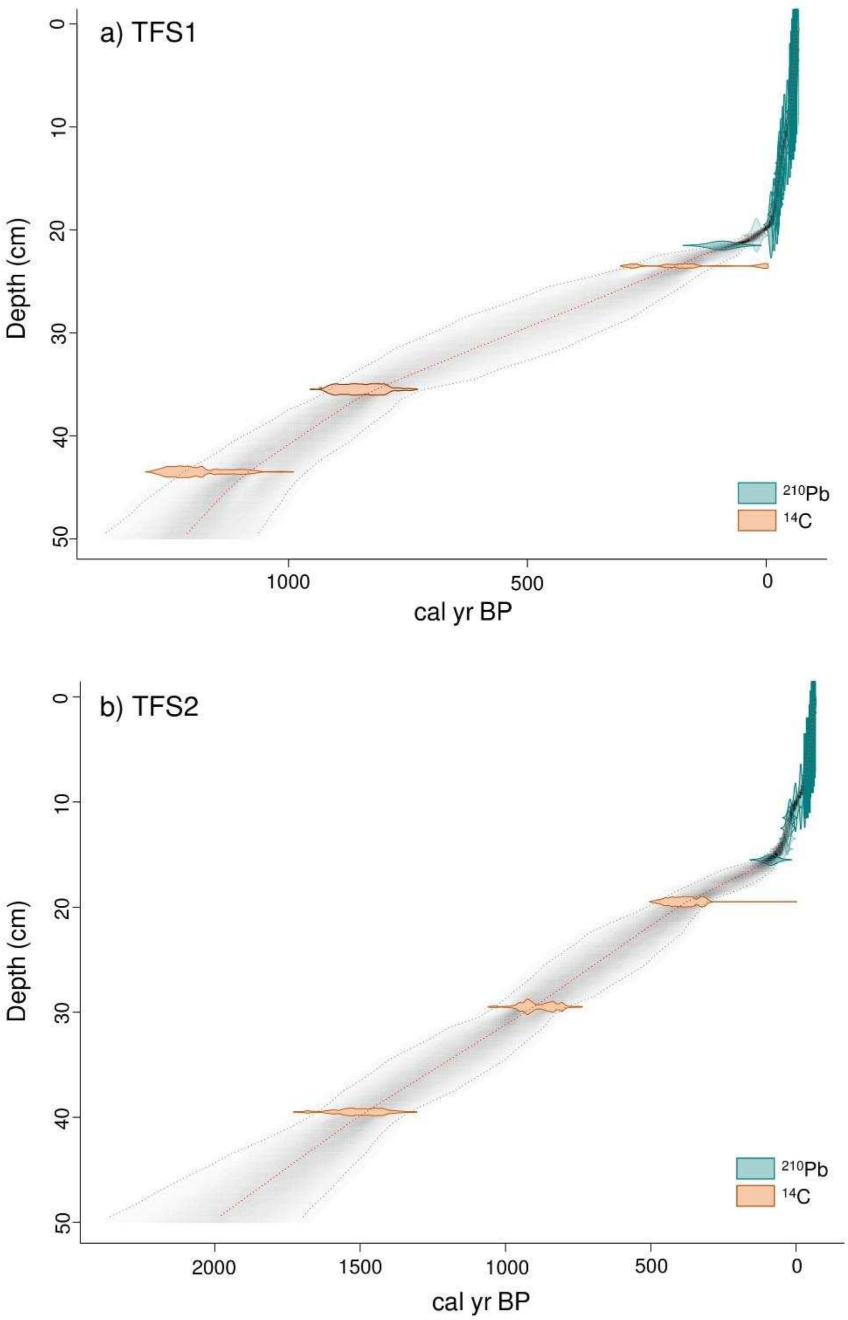


Figure 2 – Bayesian age models of (a) TFS1 and (b) TFS2.

## 3.2 Testate amoeba-based reconstructions

We use the Weighted Averaging Partial Least Squares (WAPLS) second component model presented by Taylor et al. (2019) to reconstruct WTD in both cores. Reconstructions with errors are shown alongside testate amoebae assemblages in Figures 3 and 4. TFS1 began with a high water table (Figure 5), but a rise in

Centropyxis aerophila during the Little Ice Age (LIA) indicates a rapid transition to a deeper WTD. In the last few centuries, the peatland has been dominated by Archerella flavum and Hyalosphenia papilio which indicates a moderately-wet ecosystem. TFS2 also began with a high WTD (Figure 6), but then dried rapidly as indicated by an increasing dominance of C. aerophila. Only TFS2 shows evidence of peatland initiation, given the rapid increase in organic content from LOI and transition to a deep water table that occurs at c. 200 CE. A phase dominated by Conicocassis pontigulasiformis from c. 500–1000 CE indicates a period of shallow WTD conditions. TFS2 remained fairly steady with a moderate water table for much of the past few centuries, but begun rapidly drying from c. 1850 CE, as indicated by a gradually increasing abundance of Corythion dubium, Cryptodifflugia oviformis and Assulina seminulum.

To reconstruct EC, we used a Weighted Averaging model with inverse deshrinking (WA_inv), which is a different statistical approach than the WAPLS model used by Taylor et al. (2019). This is because we found that the application of the WAPLS model led to erroneous results regarding C. pontigulasiformis, which suggested that this species was indicative of oligotrophic conditions owing to its rarity in the contemporary record and the model under fitting these data. Relatively little is known about this rare species, and it was not found regularly by Taylor et al. (2019) (but, where present, indicated minerotrophy). As C. pontigulasiformis dominates at one point in both cores, we felt it was necessary to use a model that better predicted this species and opted for WA_inv, despite it having slightly lower performance ($R^2_{BOOT}$ = 0.67, $RMSEP_{BOOT}$ = 158 μS $cm^{-1}$) than the WAPLS (Component 2) model by Taylor et al. (2019) ($R^2_{JACK}$ = 0.76, $RMSEP_{JACK}$ = 146 μS $cm^{-1}$). TFS1 remains minerotrophic for much of the duration of the core, before transitioning rapidly to oligotrophy around 1950 CE. TFS2 is more varied and appears to include two short-lived shifts to more oligotrophic states (c. 400 CE and c. 1300 CE), both followed quickly by returns to minerotrophic conditions, before the full transition to the peatland's current oligotrophic state at ~1850 CE.

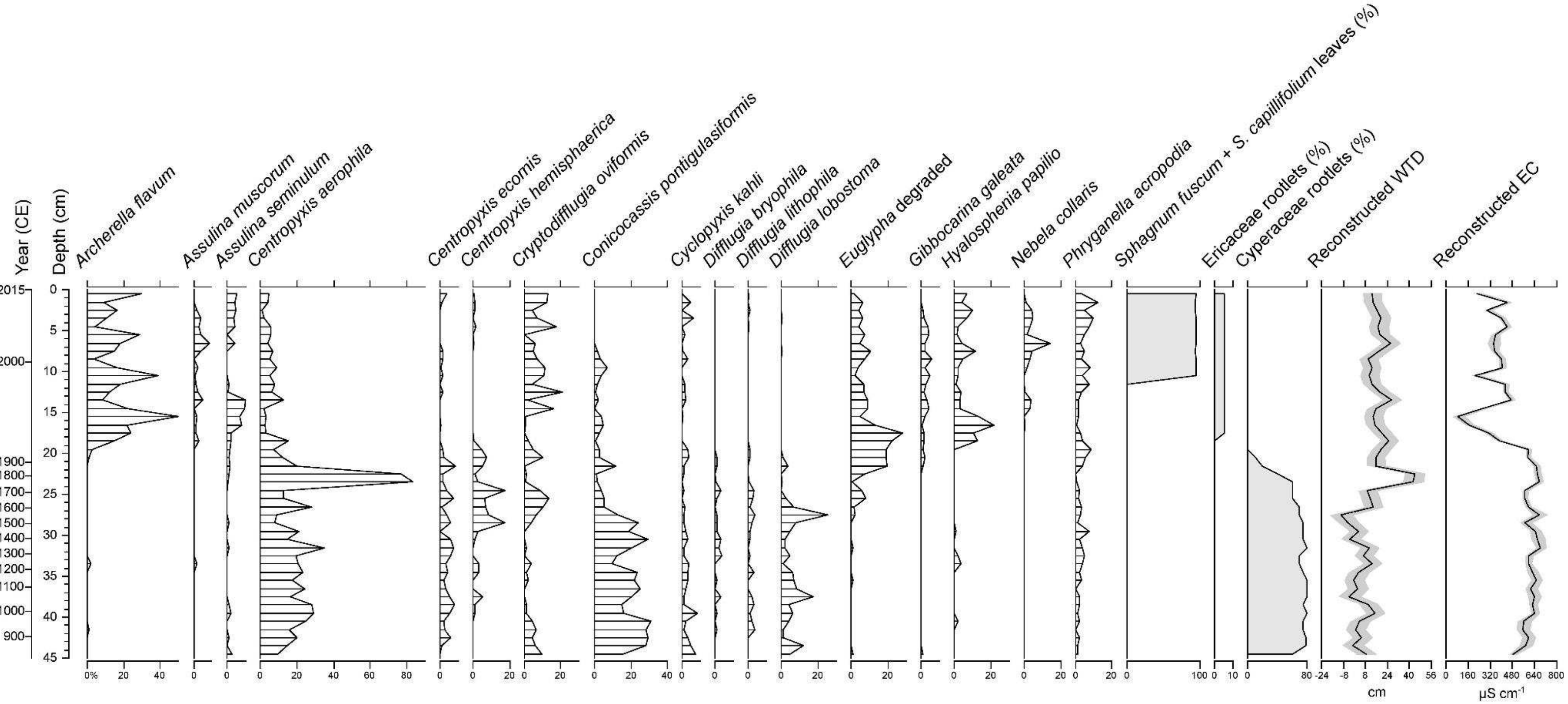


Figure 3 – Testate amoebae assemblages of TFS1*, with selected macrofossil assemblages from Gałka et al. (2018)*. WTD and EC reconstructions with standard errors (shown in grey shading) are also presented.

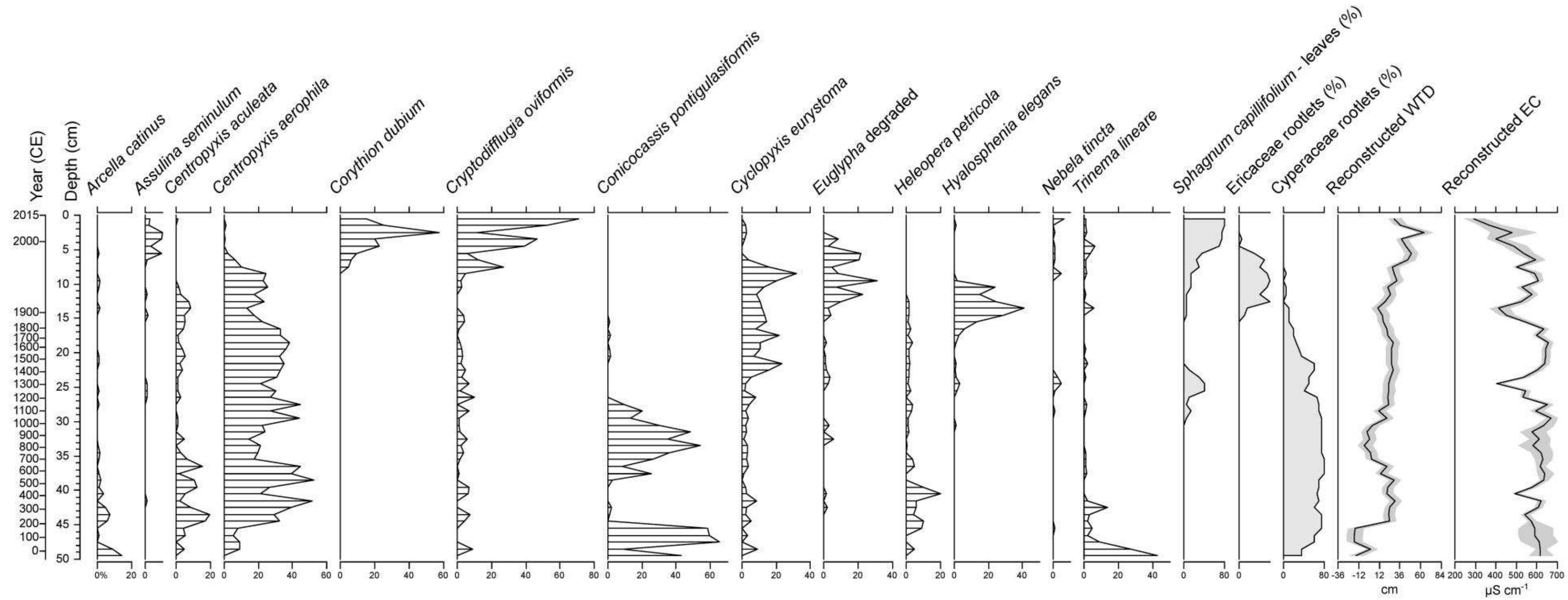


Figure 4 – Testate amoebae assemblages of TFS2*, with selected macrofossil assemblages from Gałka et al. (2018)*. WTD and EC reconstructions with standard errors (shown in grey shading) are also presented.

### 3.3 Bulk Density, Loss-on-ignition and carbon accumulation

At the base of TFS1, BD is high (0.27 g $cm^{-3}$) and LOI is low (69%). A rapid increase in BD to 0.38 g $cm^{-2}$ and a decrease in LOI to 32% between 32.5 and 29.5 cm (corresponding to 1250–1400 CE) reflects an anomalously large amount of fine-grained minerogenic material. BD and LOI return to their previous levels after this event, before BD declines rapidly and LOI increases rapidly in the early 1950s. Carbon accumulation rate was low throughout most of the core, slightly decreasing throughout the late-Holocene before rapid acceleration in the early 1900s (Figure 5).

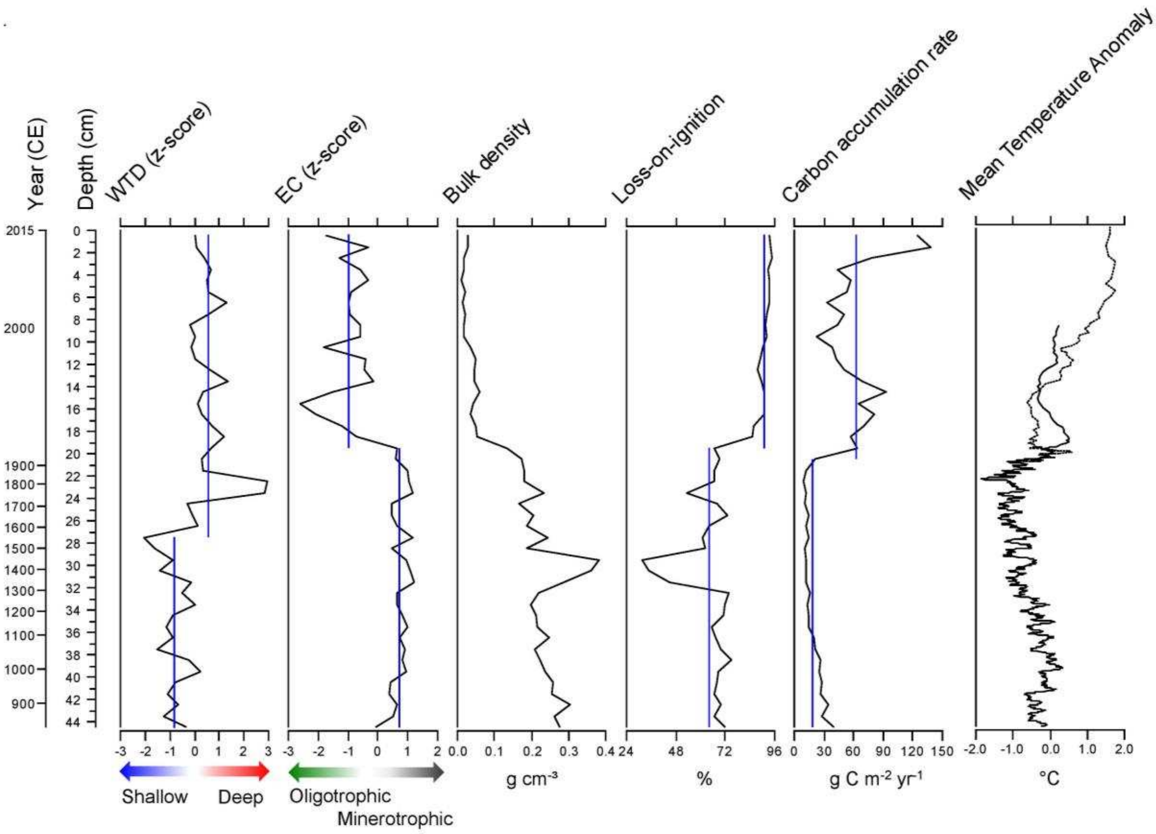


Figure 5 – Full reconstruction of palaeoenvironmental variables for TFS1. Blue lines represent mean values of samples before and after the change point. 10-year moving average temperature anomaly is relative to a 1961-1990 baseline for both PAGES2K (solid line; 0 – 2000 CE) and CRU TS (dotted line; 1901 – 2015 CE).

In TFS2, a rapid increase in LOI (representing a rise in estimated organic matter content; from 34% to 52%) at around 200 CE is a clear indication of peatland initiation. An anomalous peak in BD of 1.05 g $cm^{-3}$ at 46.5 cm corresponds to a rock clast within the peat matrix, possibly derived from the basal glacial sediments. As with TFS1, BD and LOI remain fairly constant throughout the late-Holocene, with carbon accumulation decreasing very gradually over time. The transition to more rapid carbon accumulation, low BD and rising LOI comes earlier in TFS2, at approximately 1850 CE (Figure 6).

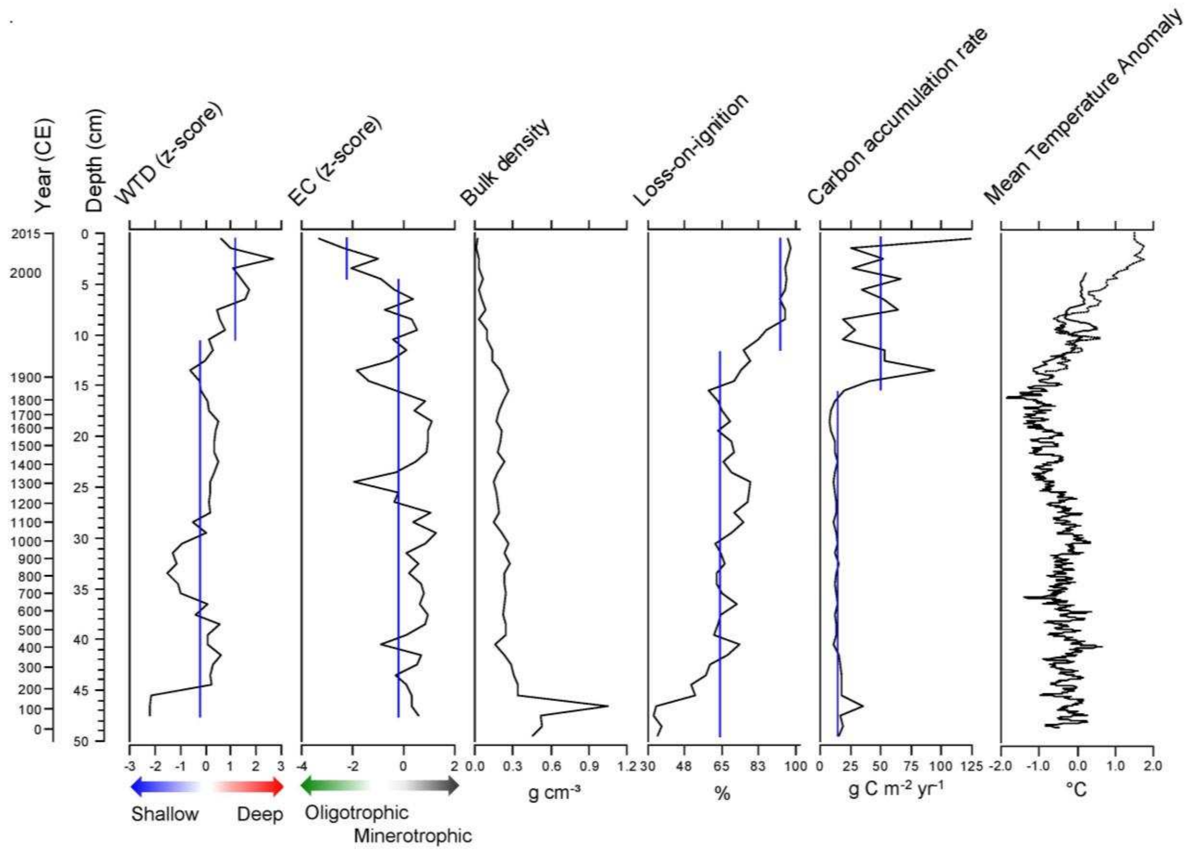


Figure 6 – Full reconstruction of palaeoenvironmental variables for TFS2. Blue lines represent mean values of samples before and after the change point. 10-year moving average temperature anomaly is relative to a 1961-1990 baseline for both PAGES2K (solid line; 0 – 2000 CE) and CRU TS (dotted line; 1901 – 2015 CE).

### 3.4 Relationship to climate data

High-precision $^{210}Pb$ analysis allows us to investigate if there has been any correlation between recent changes (from 1900 CE) in the peatland and shifts in the climate. We tested the correlations between WTD, EC and CAR against annual and seasonal temperature and precipitation records. TFS1 showed a strong positive correlation between CAR and annual, summer and autumn precipitation ($p < 0.01$; $r = 0.623$, 0.552 and 0.701 respectively); no other relationships were significant in TFS1. TFS2 showed significant positive correlations between WTD and annual, summer, spring and July temperature ($r = 0.673$, 0.771, 0.678 and 0.804 respectively; $p < 0.01$ in all cases). Although these climate variables correlate with observed changes in the peatlands, this does not necessarily infer they are the primary drivers of change, given the complex connectivity of peatland drivers.

We also investigated whether these relationships had remained stationary through time. Increasing chronological errors in deeper layers of both cores prevented the meaningful application of correlation analyses along their entire lengths. Instead we use a change point analysis to identify when the biggest transitions of WTD, EC, LOI and CAR occurred. This allows us to evaluate whether sudden, rapid warming has given rise to similar transitions in the dynamics of the peatlands. The most significant change in EC, LOI and CAR occurred after 1850 CE (Table 2). In TFS1, the most significant WTD change occurs during the LIA as the peatland rapidly dries, while in TFS2, the most significant WTD change point occurred as the peatland dried post 1900 CE.

| | TFS1 | | | TFS2 | | |
|---|---|---|---|---|---|---|
| | Change point Depth (cm) | Year CE (min-max range) | Transition Description | Change point Depth (cm) | Year CE (min-max range) | Transition Description |
| WTD | 27.5 | 1555 (1383–1702) | Drier | 10.5 | 1940 (1930–1951) | Drier |
| EC | 19.5 | 1959 (1952–1965) | Towards oligotrophy | 4.5 | 1997 (1993–2001) | Towards oligotrophy |
| LOI | 19.5 | 1959 (1952–1965) | Increase | 11.5 | 1930 (1922–1938) | Increase |
| CAR | 20.5 | 1930 (1916–1944) | Increase | 15.5 | 1853 (1816–1886) | Increase |

Table 2 - Change point analysis showing timing of the most significant changes in each reconstructed variable in the two cores.

## 4. Discussion

This study highlights the usefulness of testate amoeba-based reconstructions to identify ecosystem state shifts in peatlands in the continuous permafrost zone. Our results are similar to the observed increase in carbon accumulation of other permafrost peatlands post-1850 CE (Yu et al., 2009; Lamarre et al., 2012; Loisel and Yu, 2013), in addition to identifying an ecosystem shift in both cores towards oligotrophic fens with deep water tables.

### 4.1 Testate amoebae analysis

Our 1 cm resolution testate amoeba analysis is comparable to the lower resolution (4 cm) study on core TFS2 by Gałka et al. (2018). Their study comprised of a semi-quantitative analysis of wetness indicators, as no suitable transfer function existed at that time. While our analysis largely supports theirs, there are notable differences in taxa in the deepest sections, and throughout the core for small taxa (e.g. C. oviformis). We hypothesise that these differences occur due to the methods used to isolate the tests. We placed peat sub-samples in freshly boiled water which was allowed to cool for 10-minutes, compared to Gałka et al. (2018) placing sub-samples in continuously boiling water. This may have degraded their tests and contributed to lower observed species diversity, particularly in the deepest samples. We identified C. pontigulasiformis at significant abundance (max. 65.2%) in both fossil records, with a trend of increasing abundance with depth. This contrasts with the contemporary counts of this species, which are limited (Taylor et al., 2019). Similar records of C. pontigulasiformis also show this species to be relatively rare in the contemporary record (Beyens et al., 1986; Beyens and Chardez, 1995; Gavel et al., 2018), but have been reported in sub-Arctic lakes (Nasser and Patterson, 2015).

### 4.2 Peatland initiation

Peatlands across the Alaskan North Slope began to initiate around 8,600 years ago (Jones and Yu, 2010), likely during warm periods (MacDonald et al., 2006; Gorham et al., 2007) as a result of increased plant productivity (Morris et al., 2018). Only TFS2 shows evidence of peat initiation at the base of the core, corresponding to ~200 CE. Hu et al. (2001) note that Alaska experienced a warm period between 0 and 300 CE, which we hypothesise initiated peat accumulation in TFS2. Initiation in TFS2 is also identified in macrofossil analysis (Gałka et al. 2018), with Cyperaceae (mainly Carex species) and herb rootlets increasing steadily between 48.5 and 46.5 cm, during the 0-300 CE warm period.

### 4.3 Post-initiation development

The presence of Difflugia lobostoma gradually increases in TFS1 between 800 CE and 1600 CE, indicating WTD becoming steadily shallower during this period. Between 32.5 and 29.5 cm (corresponding to ~1250-1400 CE), LOI dramatically falls (from 73% to 32%), BD rises (from 0.22 to 0.38 g $cm^{-3}$) and a large quantity of minerogenic material (mainly quartz) is found in the samples. TFS1 was extracted close to Toolik Lake and is 9 m lower in elevation than TFS2. We hypothesise that this anomaly is a result of the lake briefly rising to flood the peatland before subsequently falling. Given the 150-year time range that this event corresponds to, this could signify lake level change over a number of decades, or a shorter event that resulted in greater sediment deposition. We do not observe any change in testate amoebae assemblage, so we hypothesise that this was caused by a much shorter event that briefly raised lake level than a longer-term, multi-decadal rise, as testate amoebae have a life span of a matter of days (Wilkinson and Mitchell, 2010).

In TFS2, a period of wetter, minerotrophic conditions centres on 800 CE. This period is indicated by a peak in C. pontigulasiformis, which is also observed at the same time in TFS1 (although C. pontigulasiformis remains present for longer in TFS1). Climate drivers may have been responsible for lowering WTD, as the region experienced a warm period from 850-1200 CE (Hu et al., 2001) which corresponds to steadily drier conditions in TFS2, although this is not observed in TFS1. The transition back to dryness is indicated by a resurgence of C. aerophila and an increasing abundance of Phryganella acropodia.

### 4.4 Little Ice Age (LIA)

In TFS1, there is a notable shift towards drier conditions beginning approximately 1550 CE, during the LIA (1400-1700 CE; Mann et al., 2009). This dry shift is indicated by a large spike in C. aerophila (peaking at 83% abundance). During this period, LOI, BD and CAR remain steady and both peatlands are minerotrophic. TFS2 does not exhibit a shift towards dryness, likely because WTD was already deep (as indicated by Centropyxis platystoma and C. aerophila). However, both cores exhibit a wetting trend at the end of the LIA. Testate-amoeba based reconstructions from permafrost peatlands in Canada (Lamarre et al., 2012), Finland and Russia (Zhang et al., 2018) also show drier conditions during the LIA. This may be due to permafrost aggradation elevating the surface (Zoltai, 1993). A $\delta^{18}O$ record from the south-central Brooks Range indicates that the LIA may have caused an increase in precipitation in the winter and a decrease in summer (Clegg and Hu, 2010), allowing the water table to fall and the peat to dry during the growing season.

### 4.5 Industrial Revolution

As TFS1 recovers from the LIA in the late 1800s, WTD remains relatively steady at a moderate depth, with increasing oligotrophy and carbon accumulation. This is evidenced by a switch towards dominance by A. flavum, H. papilio and Nebela collaris among others. CAR rapidly accelerates at the start of the twentieth century. Change point analysis shows that the most notable shift in CAR occurs after 1850 CE, from a mean of 18.4 g C $m^{-2}$ $yr^{-1}$ before, to a mean of 59.5 g C $m^{-2}$ $yr^{-1}$ as temperatures rise across the region.

In TFS2, CAR begins to rapidly increase at c. 1850 CE, as the peatland shifts to become gradually drier and more oligotrophic. C. dubium, C. oviformis and Assulina sp. are most prevalent after 1850. CAR in the top of the core is highly variable between samples. CAR changes from a mean of 14.2 g C $m^{-2}$ $yr^{-1}$ to a mean of 48.2 g C $m^{-2}$ $yr^{-1}$ after 1850 CE, with the most significant change point occurring at the very beginning of the industrial revolution. This apparent change in CAR is consistent with the hypothesis of a recent ecosystem state shift.

It is usual for peatland reconstructions to show CAR accelerating towards the top of the core, because the uppermost, oxic layer continues to decompose more rapidly than deeper peat preserved in saturated conditions (Roulet et al., 2007). However, our peatlands become both drier and more oligotrophic at the same time that CAR accelerates. Such a pattern is not characteristic of incomplete decay (Ingram, 1978), and indicates that there has been a fundamental ecosystem state shift in these peatlands in response to recent warming. Furthermore, the initial rapid increase in CAR that begins in both peatlands prior to 1900 CE occurs before a reduction in bulk density values, which suggests that the increase in CAR is not solely due to incomplete decay. Similarly rapid increases in CAR have also been observed in south-central (Loisel and Yu, 2013) and southwestern Alaska (Klein et al., 2013), with the application of decomposition models not affecting their conclusions that recent warming has increased CAR. While we cannot reject the possibility that the observed CAR increase is due to incomplete decay, concomitant changes in other characteristics of the peatlands suggest that recent warming has impacted CAR, warranting further investigation in similar peatlands across the continuous permafrost zone.

Macrofossil and pollen analysis performed on both cores (Gałka et al., 2018) also support our findings. Using the chronology presented here, we find that a large rise in Sphagnum begins in the 1940s in TFS1 and in the late 1800s in TFS2. Ericaceae rootlets also dramatically increase at a similar time, further supporting their transition to oligotrophic poor fen status (Pancost et al., 2003). Throughout late-Holocene warm periods, Gałka et al. (2018) note an increase in shrub species (Ericaceae, Andromeda polifolia and Empetrum nigrum), supporting the hypothesis that Arctic peatlands may become more productive under future warming. Nearby expansion of Sphagnum has also been linked to future warming and increased carbon sequestration (Cleary, 2015). This has also been evidenced in studies from discontinuous permafrost peatlands (e.g. Turetsky et al., 2007; Natali et al., 2012), including shrub expansion and local plant succession in sub-arctic Sweden (Gałka et al., 2017) and Sphagnum expansion driving CAR in central Alaska (Jones et al., 2012), although the long-term lasting effect of accelerated carbon accumulation has been questioned (Dise, 2009).

### 4.6 Permafrost Peatlands and Climate Change

Given that ours is the first study to quantitatively reconstruct peatland dynamics in continuous permafrost, it is challenging to identify synergy between our findings and previous works. Charman et al. (2009) identified that bog surface wetness was primarily driven by precipitation in bogs from the UK and Estonia, but they did not investigate CAR. Charman et al. (2013) found that temperature changes across the late-Holocene drive changes in CAR from a range of peatlands across Europe, but they did not investigate precipitation changes. Zhang et al. (2018) also found increasingly dry conditions in discontinuous and sporadic permafrost peatlands from across Finland and Siberia, noting that this is indicative of increased evapotranspiration. In south-central Alaska, Klein et al. (2005) also observe regional drying across wetlands in the Kenai Lowlands, corresponding to rising temperatures. The differences in the influence of climate on TFS1 and TFS2 may be due to the short analysis period (1900 - 2015 CE; compared to Charman et al. (2013) over two millennia), and slow peat accumulation rate of permafrost peatlands. Alternatively, as both peatlands are sloping, microtopography at the site may regulate the extent to which precipitation influences CAR. Where reliable daily temperature data exist, future studies in permafrost regions may also wish to investigate the influence of growing season length or growing degree days on peatland dynamics, as this has been found to influence vegetation growth (Piao et al., 2007).

Our data suggest that warming temperatures have led to increased productivity in these Arctic peatlands, which directly enhanced their recent carbon sequestration rates. However, it is unclear whether this enhanced sink can be maintained under further warming, or whether respiration will come to dominate peatland-atmosphere fluxes, causing carbon release to increase (Dorrepaal et al., 2009; Hodgkins et al., 2014; Comyn-Platt et al., 2018). Adding to the complexity of the system, the uncertainty of future permafrost peatlands and their role in the carbon cycle will be complicated by hydrological changes that result from collapse (Swindles et al., 2015b), as well as changes in vegetation, peat chemistry and organic matter quality (Treat et al., 2014). If, as seems likely, the active layer of permafrost peatlands continues to thicken, this may result in the release of carbon as $CH_4$, rather than $CO_2$, from thermokarst features (Kirkwood et al., 2018). Further analysis should now seek to identify whether our findings are representative of Arctic permafrost peatlands more generally.

## 5. Conclusions

Permafrost peatlands represent a major global store of carbon, and little is known about the stability of this store under a future warming climate, with few previous palaeoenvironmental studies and no long-term monitoring of peatlands in the continuous permafrost zone. We reconstruct late-Holocene environmental changes in two Arctic peatlands in the Alaskan North Slope. We used two testate amoeba-based transfer functions from the continuous permafrost zone to reconstruct water-table depth and porewater electrical conductivity of two Alaskan peatlands at Toolik Lake. We identify that one of these peatlands likely initiated during a warm period between 0 and 300 CE. Prior to 1850 CE, both peatlands have remained minerotrophic and with low carbon accumulation rates that reflect the slow formation of peat in permafrost regions. However, there has been a rapid transition towards oligotrophy and a three-fold increase in mean carbon accumulation rate since 1850 CE. Our results suggest that recent warming is responsible for the transition of Alaskan Arctic rich fens with low carbon accumulation to oligotrophic poor fens with an increased ability to sequester carbon. As the Arctic continues to warm, peatlands in the continuous permafrost zone may become an increasingly important carbon sink.

## Contributions

LST, GTS and PJM designed the research. GTS and MG carried out the fieldwork. LST and SMG performed $^{210}$Pb analysis. LST performed all other laboratory and climate analysis under supervision from GTS and PJM. All authors contributed to the final manuscript.

## Acknowledgements

We are grateful for support from INTERACT (grant agreement No 262693) under the European Community's Seventh Framework Programme. LST is supported in part by a bursary from the University of Leeds's Ecology and Global Change research cluster. We are thankful to Randy Fulweber, Angelica Feurdean and the staff at the Toolik Field Station, Alaska for assistance in the field. Thanks also to Angela Gallego-Sala, Mark Smith, Tom Roland and two anonymous reviewers for their helpful comments and suggestions in improving an earlier version of this manuscript.

## References

Amesbury, M.J., Roland, T.P., Royles, J. et al. 2017. Widespread Biological Response to Rapid Warming on the Antarctic Peninsula. Current Biology **27**; pp.1616-1622. https://doi.org/10.1016/j.cub.2017.04.034.

Appleby, P.G. 2001. Chronostratigraphic techniques in recent sediments. In W. M. Last and J. P. Smol (Eds.), Tracking Environmental Change Using Lake Sediments Volume 1: Basin Analysis, Coring and Chronological Techniques (pp. 171-203). Dordrecht, Klower Academic Publishers.

Appleby, P.G. and Oldfield, F. 1978. The calculation of lead-210 dates assuming a constant rate of supply of unsupported $^{210}$Pb to the sediment. Catena **5**; pp.1-8. https://doi.org/10.1016/S0341-8162(78)80002-2

Beaulieu-Andy, V., Garneau, M., Richard, P.J.H. and Asnong, H. 2009. Holocene Palaeoecological reconstruction of three boreal peatlands in the La Grande Rivière region, Québec, Canada. The Holocene **19**; pp.459-476. https://doi.org/10.1177%2F0959683608101395

Bellamy, P.H., Loveland, P.J., Bradley, R.I. et al. 2005. Carbon losses from all soils across England and Wales 1978-2003. Nature **437**; pp.245-248. https://doi.org/10.1038/nature04038

Beyens, L. and Chardez, D. 1995. An annotated list of testate amoebae observed in the Arctic between the longitudes 27˚E and 168˚W. Archiv für Protistenkunde **146**; pp.219-233. https://doi.org/10.1016/S0003-9365(11)80114-4.

Beyens, L., Chardez, D. and DeBock, P. 1986. Some new and rare testate amoebae from the Arctic. Acta Protozoologica **25**; pp.81-91.

Blaauw, M., Christen, J.A., Vazquez, J.E., et al. 2018. rbacon: Age-Depth Modelling using Bayesian Statistics, R package version 2.3.4. [Online] https://CRAN.R-project.org/package=rbacon.

Booth, R.K., Lamentowicz, M. and Charman, D.J. 2010. Preparation and analysis of testate amoebae in peatland palaeoenvironmental studies. Mires and Peat **7**: Art. 2. [Online] http://www.mires-and-peat.net/pages/volumes/map07/map0702.php.

Booth, R.K. and Sullivan, M. 2007. Key of Testate Amoebae Inhabiting Sphagnum-dominated Peatlands with an Emphasis on Taxa Preserved in Holocene Sediments, Lehigh University, Bethlehem.

Brown, J. 1998. Circumpolar Active-Layer Monitoring (CALM) Program: Description and data. In Circumpolar active-layer permafrost system, version 2.0. (ed.) M. Parsons and T. Zhang, (comp.) International Permafrost Association Standing Committee on Data Information and Communication. Boulder, CO: National Snow and Ice Data Center.

Charman, D.J., Beilman, D.W., Blaauw, M., et al. 2013. Climate-related changes in peatland carbon accumulation during the last millennium. Biogeosciences **10**; pp.929-944. https://doi.org/10.5194/bg-10-929-2013.

Charman, D.J., Barber, K.E., Blaauw, M., et al. 2009. Climate drivers for peatland palaeoclimate records. Quaternary Science Reviews **28**; pp.1811-1819. https://doi.org/10.1016/j.quascirev.2009.05.013.

Charman, D.J., Brown, A.D., Hendon, D. and Karofeld, E. 2004. Testing the relationship between Holocene peatland palaeoclimate reconstructions and instrumental data at two European sites. Quaternary Science Reviews **23**; pp.137-143. https://doi.org/10.1016/j.quascirev.2003.10.006.

Charman, D.J., Hendon, D. and Woodland, W.A. 2000. The Identification of Testate Amoebae (Protozoa: Rhizopoda) in Peats, Quaternary Research Association, Oxford.

Cleary, K. 2015. Shrub Expansion, Sphagnum Peat Growth, and Carbon Sequestration in Arctic Tundra on the North Slope of Alaska. Theses and Dissertations. **2557**. http://preserve.lehigh.edu/etd/2557

Clegg, B.F., and Hu, F.S. 2010. An oxygen-isotope record of Holocene climate change in the south-central Brooks Range, Alaska. Quaternary Science Reviews **29**; pp.928-939. https://doi.org/10.1016/j.quascirev.2009.12.009.

Comyn-Platt, E., Hayman, G., Huntingford, C., et al. 2018. Carbon budgets for 1.5 and 2˚C targets lowered by natural wetland and permafrost feedbacks. Nature Geoscience **11**; pp.568-573. https://doi.org/10.1038/s41561-018-0174-9.

Dise, N.B. 2009. Peatland Response to Global Change. Science **326**; pp.810-811. https://doi.org/10.1126/science.1174268.

Dorrepaal, E., Toet, S., van Logtestijn, R.S.P., et al. 2009. Carbon respiration from subsurface peat accelerated by climate warming in the subarctic. Nature **460**; pp.616-619. https://doi.org/10.1038/nature08216.

Environmental Data Center Team. 2018. Meterological monitoring program at Toolik, Alaska. Toolik Field Station, Institute of Arctic Biology, University of Alaska Fairbanks, Fairbanks, AK 99775. [Online] http://toolik.alaska.edu/edc/abiotic_monitoring/data_query.php

Flynn, W.W. 1968. The determination of low levels of polonium-210 in environmental materials. Analytica Chimica Acta **43**; pp.221-227. https://doi.org/10.1016/S0003-2670(00)89210-7

Gałka, M., Swindles, G.T., Szal, M., et al. 2018. Response of plant communities to climate change during the late Holocene: Palaeoecological insights from peatlands in the Alaskan Arctic. Ecological Indicators **85**; pp.525-536. https://doi.org/10.1016/j.ecolind.2017.10.062

Gałka, M., Szal, M., Watson, E.J., et al. 2017. Vegetation succession, carbon accumulation and hydrological change in sub-Arctic peatlands (Abisko, northern Sweden), Permafrost and Periglacial Process **28**; pp.589-604. https://doi.org/10.1002/ppp.1945

Gallego-Sala, A.V., Charman, D.J., Brewer, S. et al. 2018. Latitudinal limits to the predicted increase of the peatland carbon sink with warming. Nature Climate Change. 1758-6798. https://doi.org/10.1038/s41558-018-0271-1.

Gavel, M.J., Patterson, R.T., Nasser, N.A., et al. 2018. What killed Frame Lake? A precautionary tale for urban planners. PeerJ **6**; e4850. https://doi.org/10.7717/peerj.4850

Gorham, E., Lehman, C., Dyke, A., et al. 2007. Temporal and spatial aspects of peatland initiation following deglaciation in North America. Quaternary Science Reviews **26**; pp.300-311. https://doi.org/10.1016/j.quascirev.2006.08.008

Harris, I., Jones, P.D., Osborn, T.J., et al. 2014. Updated high-resolution grids of monthly climatic observations- the CRU TS3.10 Dataset. International Journal of Climatology **34**; pp.623-642. https://doi.org/10.1002/joc.3711.

Hodgkins, S.B., Tfaily, M.M., McCalley, C.K., et al. 2014. Changes in peat chemistry associated with permafrost thaw increase greenhouse gas production. PNAS **111**; pp.5819-5824. https://doi.org/10.1073/pnas.1314641111.

Hu, F.S., Ito, E., Brown, T.A., et al. 2001. Pronounced climatic variations in Alaska during the last two millennia. PNAS **98**; pp.10552-10556. https://doi.org/10.1073/pnas.181333798

Ingram, H.A.P. 1978. Soil Layers in Mires: Function and Terminology. Journal of Soil Science **29**; pp.224-227. https://doi.org/10.1111/j.1365-2389.1978.tb02053.x

Ise, T., Dunn, A.L., Wofsy, S.C. and Moorcroft, P.R. 2008. High sensitivity of peat decomposition to climate change through water-table feedback. Nature Geoscience **1**; pp.763-766. https://doi.org/10.1038/ngeo331

Jones, M.C., Booth, R.K., Yu, Z. and Ferry, P. A 2200-Year Record of Permafrost Dynamics and Carbon Cycling in a Collapse-Scar Bog, Interior Alaska. Ecosystems **16**; pp.1-19. https://doi.org/10.1007/s10021-012-9592-5

Jones, M.C., and Yu, Z. 2010. Rapid deglacial and early Holocene expansion of peatlands in Alaska. PNAS **107**; pp.7347-7352. https://doi.org/10.1073/pnas.0911387107

Khvorostyanov, D.V., Ciais, P., Krinner, G., et al. 2008. Vulnerability of east Siberia’s frozen carbon stores to future warming. Geophysical Research Letters **35**; L10703. https://doi.org/10.1029/2008GL033639

Killick, R., Haynes, K., Eckley, I., et al. 2016. Changepoint: Methods for Changepoint Detection, R package version 2.2.2. [Online] https://cran.r-project.org/package=changepoint

Kirkwood, A.H., Roy-Léveillée, P., Basiliko, N., et al. 2018. Microbial greenhouse gas production in permafrost peatlands of the Hudson Bay Lowlands, Canada. 5th European Conference on Permafrost, Chamonix, June 2018.

Klein, E.S., Yu, Z. and Booth, R.K. 2013. Recent increase in peatland carbon accumulation in a thermokarst lake basin in southwestern Alaska. Palaeogeography, Palaeoclimatology, Palaeoecology **392**; pp.186-195. https://doi.org/10.1016/j.palaeo.2013.09.009

Klein, E.S., Berg, E.E. and Dial, R. 2005. Wetland drying and succession across the Kenai Peninsula Lowlands, south-central Alaska. Canadian Journal of Forest Research **35**; pp.1931-1941. https://doi.org/10.1139/x05-129

Lamarre, A., Garneau, M. and Asnong, H. 2012. Holocene paleohydrological reconstruction and carbon accumulation of a permafrost peatland using testate amoeba and macrofossil analyses, Kuujjuarapik, subarctic Québec, Canada. Review of Palaeobotany and Palynology **186**; pp.131-141. https://doi.org/10.1016/j.revpalbo.2012.04.009

Langdon, P.G. and Barber, K.E. 2005. The climate of Scotland over the last 5000 years inferred from multiproxy peatland records: inter-site correlations and regional variability. Journal of Quaternary Science **20**; pp.549-566. https://doi.org/10.1002/jqs.934

Loisel, J. and Yu, Z. 2013. Recent acceleration of carbon accumulation in a boreal peatland, south central Alaska. Biogeosciences **118**; pp.41-53. https://doi.org/10.1029/2012JG001978

MacDonald, G.M., Beilman, D.W., Kremenetski, K.V., et al. 2006. Rapid Early Development of Circumarctic Peatlands and Atmospheric $CH_4$ and $CO_2$ Variations. Science **314**; pp.285-288. https://doi.org/10.1126/science.1131722.

Mann, M.E., Zhang, Z. and Rutherford, S. 2009. Global Signatures and Dynamical Origins of the Little Ice Age and Medieval Climate Anomaly. Science **326**; pp.1256-1260. https://doi.org/10.1126/science.1177303.

Moore, T.R., Roulet, N.T. and Waddington, J.M. 1998. Uncertainty in Predicting the Effect of Climatic Change on the Carbon Cycling of Canadian Peatlands. Climatic Change **40**; pp.229-245. https://doi.org/10.1023/A:1005408719297.

Morris, P.J., Swindles, G.T., Valdes, P.J., et al. 2018. Global peatland initiation driven by regionally asynchronous warming. PNAS **115**; pp.4851-4856. https://doi.org/10.1073/pnas.1717838115

Nasser, N.A. and Patterson, R.T. 2015. Conicocassis, a new genus of Arcellinina (testate lobose amoebae). Palaeontologia Electronica **18**; pp.1-11. https://doi.org/10.26879/538

Natali, S.M., Schuur, E.A.G. and Rubin, R.L. 2012. Increased plant productivity in Alaskan tundra as a result of experimental warming of soil and permafrost. Journal of Ecology **100**; pp.488-498. https://doi.org/10.1111/j.1365-2745.2011.01925.x.

PAGES2k Consortium. 2017. A global multiproxy database for temperature reconstructions of the Common Era. Scientific Data, 4, 170088. https://doi.org/10.1038/sdata.2017.88

Pancost, R.D., Baas, M., van Geel, B., et al. 2003. Response of an ombrotrophic bog to a regional climate event revealed by macrofossil, molecular and carbon isotopic data. The Holocene **13**; pp.921-932. https://doi.org/10.1191/0959683603hl674rp

Piao, S., Friedlingstein, P., Ciais, P., et al. 2007. Growing season extension and its impact on terrestrial carbon cycle in the Northern Hemisphere over the past 2 decades. Global Biogeochemical Cycles **21**; GB3018. https://doi.org/10.1029/2006GB002888

R Core Team. 2014. R: A language and environment for statistical computing, R Foundation for Statistical Computing, Vienna, Austria. [Online] http://www.R-project.org.

Roulet, N.T., Lafleur, P.M., Richard, P.J.H., et al. 2007. Contemporary carbon balance and late Holocene carbon accumulation in a northern peatland. Global Change Biology **13**; pp.397-411. https://doi.org/10.1111/j.1365-2486.2006.01292.x

Schaefer, K., Zhang, T., Bruhwiler, L., et al. 2011. Amount and timing of permafrost carbon release in response to climate warming. Tellus **63**; pp.165-180. https://doi.org/10.1111/j.1600-0889.2011.00527.x

Schuur, E.A.G., Abbott, B.W., Bowden, W.B., et al. 2013. Expert assessment of vulnerability of permafrost carbon to climate change. Climatic Change **119**; pp.359-374. https://doi.org/10.1007/s10584-013-0730-7

Schuur, E.A.G., Bockheim, J., Canadell, J.G., et al. 2008. Vulnerability of Permafrost Carbon to Climate Change: Implications for the Global Carbon Cycle. BioScience **58**; pp.701-714. https://doi.org/10.1641/B580807

Siemensma, F.J. 2018. Microworld, world of amoeboid organisms, Kortenhoef, Netherlands [Online] https://www.arcella.nl.

Sillasoo, U., Mauquoy, D., Blundell, A., et al. 2007. Peat multi-proxy data from Männikjärve bog as indicators of late Holocene climate changes in Estonia. BOREAS **36**; pp.20-37. https://doi.org/10.1111/j.1502-3885.2007.tb01177.x

Swindles, G.T., Amesbury, M.J., Turner, T.E., et al. 2015a. Evaluating the use of testate amoebae for palaeohydrological reconstruction in permafrost peatlands. Palaeogeography, Palaeoclimatology, Palaeoecology **424**; pp.111-122. https://doi.org/10.1016/j.palaeo.2015.02.004

Swindles, G.T., Morris, P.J., Mullan, D., et al. 2015b. The long-term fate of permafrost peatlands under rapid climate warming. Scientific Reports **5**; 17951. https://doi.org/10.1038/srep17951.

Swindles, G.T., Blaauw, M., Blundell, A. and Turner, T.E. 2012. Examining the uncertainties in a 'tuned and stacked' peatland water table reconstruction. Quaternary International **268**; pp. 58-64. https://doi.org/10.1016/j.quaint.2011.04.029

Swindles, G.T., Blundell, A., Roe, H.M., et al. 2010. A 4500-year proxy climate record from peatlands in the North of Ireland: the identification of widespread summer 'drought phases'?. Quaternary Science Reviews **29**; pp.1577-1589. https://doi.org/10.1016/j.quascirev.2009.01.003

Swindles, G.T., Plunkett, G. and Roe, H.M. 2007. A multiproxy climate record from a raised bog in County Fermanagh, Northern Ireland: a critical examination of the link between bog surface wetness and solar variability. Journal of Quaternary Science **22**; pp.667-679. https://doi.org/10.1002/jqs.1093

Tarnocai, C., Canadell, J.G., Schuur, E.A.G., et al. 2009. Soil organic carbon pools in the northern circumpolar permafrost region. Global Biogeochecmical Cycles **23**; GB2023. https://doi.org/10.1029/2008GB003327.

Taylor, L.S., Swindles, G.T., Morris, P.J. and Gałka, M. 2019. Ecology of peatland testate amoebae in the Alaskan continuous permafrost zone. Ecological Indicators **96**; pp.153-162. https://doi.org/10.1016/j.ecolind.2018.08.049.

Treat, C.C., Wollheim, W.M., Varner, R.K., et al. 2014. Temperature and peat type control $CO_2$ and $CH_4$ production in Alaskan permafrost peats. Global Change Biology **20**; pp.2674-2686. https://doi.org/10.1111/gcb.12572.

Turetsky, M.R., Wieder, R.K., Vitt, D.H., et al. 2007. The disappearance of relict permafrost in boreal north America: Effects on peatland carbon storage and fluxes. Global Change Biology **13**; pp.1922-1934. https://doi.org/10.1111/j.1365-2486.2007.01381.x

Wilkinson, D.M. and Mitchell, E.A.D. 2010. Testate Amoebae and Nutrient Cycling with Particular Reference to Soils. Geomicrobiology Journal **27**; pp.520-533. https://doi.org/10.1080/01490451003702925

Woodland, W.A., Charman, D.J. and Sims, P.C. 1998. Quantitative estimates of water tables and soil moisture in Holocene peatlands from testate amoebae. The Holocene **8**; pp.261-273. https://doi.org/10.1191%2F095968398667004497.

Yu, Z., Beilman, D.W. and Jones, M.C. 2009. Sensitivity of Northern Peatland Carbon Dynamics to Holocene Climate Change. Geophysical Monograph Series **184**; pp.55-69. https://doi.org/10.1029/2008GM000822.

Zhang, H., Piilo, S.R., Amesbury, M.J., et al. 2018. The role of climate change in regulating Arctic permafrost peatland hydrological and vegetation change over the last millennium. Quaternary Science Reviews **182**; pp.121-130. https://doi.org/10.1016/j.quascirev.2018.01.003.

Zoltai, S.C. 1993. Cyclic development of permafrost in the peatlands of Northwestern Alberta, Canada. Arctic and Alpine Research **25**; pp.240-246. https://doi.org/10.1080/00040851.1993.12003011

# Appendix A

## $^{210}$Pb Data and Activity Profiles – TFS1

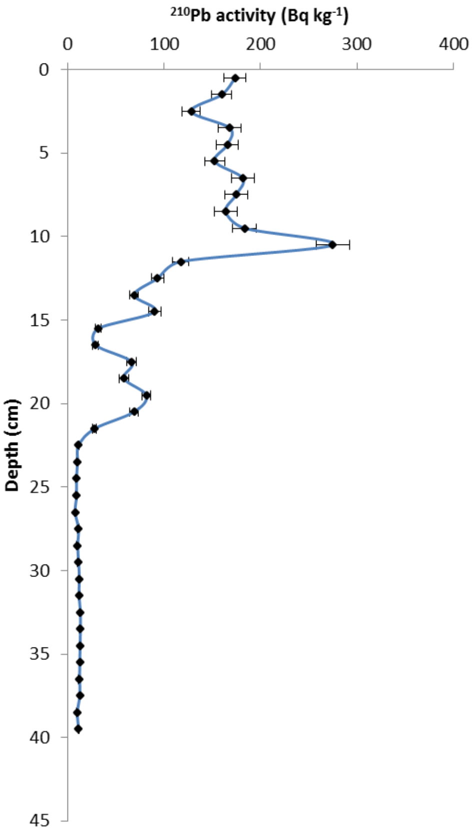


| Depth (cm) | Age (year) | ± |
|---|---|---|
| 0.5 | 0.64 | 1.02 |
| 1.5 | 2.03 | 1.08 |
| 2.5 | 2.72 | 1.16 |
| 3.5 | 3.55 | 1.18 |
| 4.5 | 4.59 | 1.21 |
| 5.5 | 6.93 | 1.27 |
| 6.5 | 8.56 | 1.36 |
| 7.5 | 11.47 | 1.44 |
| 8.5 | 13.10 | 1.51 |
| 9.5 | 15.14 | 1.56 |
| 10.5 | 20.08 | 1.71 |
| 11.5 | 26.31 | 1.90 |
| 12.5 | 29.64 | 1.99 |
| 13.5 | 33.21 | 2.11 |
| 14.5 | 36.81 | 2.24 |
| 15.5 | 38.58 | 2.28 |
| 16.5 | 39.70 | 2.33 |
| 17.5 | 42.12 | 2.44 |
| 18.5 | 48.05 | 2.71 |
| 19.5 | 54.38 | 2.99 |
| 20.5 | 84.89 | 6.23 |
| 21.5 | 156.87 | 23.14 |

## $^{210}$Pb Data and Activity Profiles – TFS2

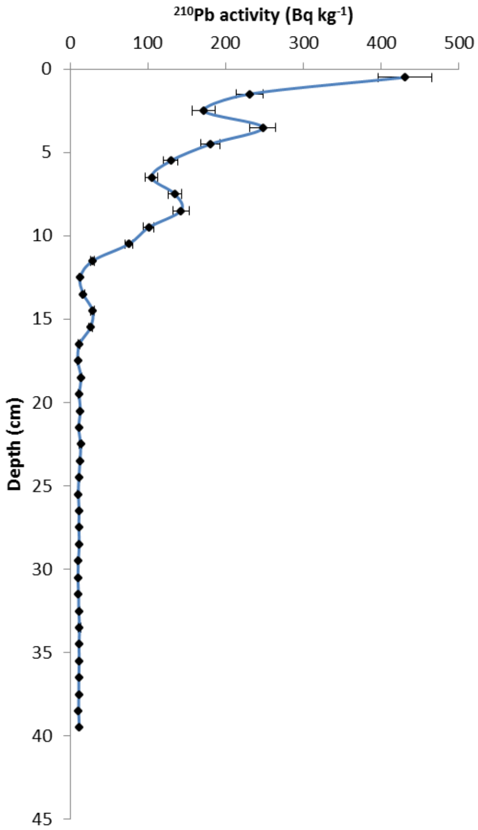


| Depth (cm) | Age (year) | ± |
|---|---|---|
| 0.5 | 1.66 | 1.05 |
| 1.5 | 3.58 | 1.21 |
| 2.5 | 6.43 | 1.30 |
| 3.5 | 9.90 | 1.45 |
| 4.5 | 16.12 | 1.70 |
| 5.5 | 19.75 | 1.85 |
| 6.5 | 23.63 | 1.98 |
| 7.5 | 31.34 | 2.30 |
| 8.5 | 35.66 | 2.37 |
| 9.5 | 49.25 | 3.10 |
| 10.5 | 67.97 | 4.27 |
| 11.5 | 86.31 | 5.63 |
| 12.5 | 91.42 | 5.96 |
| 13.5 | 94.92 | 6.26 |
| 14.5 | 112.96 | 9.33 |
| 15.5 | 152.55 | 19.59 |